Journal of ELECTRICAL ENGINEERING, VOL. 62, NO. 4, 2011, 220–226

CALCULATION AND MEASUREMENT OF COIL INDUCTANCE PROFILE IN TUBULAR LINEAR RELUCTANCE MOTOR AND ITS VALIDATION BY THREE DIMENSIONAL FEM

Ali MOSALLANEJAD — Abbas SHOULAIE *

This paper reports a study of coil inductance profile in all positions of plunger in tubular linear reluctance motors (TLRMs) with open type magnetic circuits. In this paper, maximum inductance calculation methods in winding of tubular linear reluctance motors are described based on energy method. Furthermore, in order to calculate the maximum inductance, equivalent permeability is measured. Electromagnetic finite-element analysis for simulation and calculation of coil inductance in this motor is used. Simulation results of coil inductance calculation using 3-D FEM with coil current excitation is compared to theoretical and experimental results. The comparison yields a good agreement.

K e y w o r d s: tubular linear reluctance motors, maximum inductance, inductance profile, FEM analyzes

1 INTRODUCTION

Linear Motors have been widely studied using the electric circuit theory [1–5]. The linear reluctance motors were considered under both ac and dc supply. Although the ac motors have lower efficiency than the dc ones, they are employed in many applications [6]. The linear motors differ in both construction and type. One of the known motors in the group of linear motors is tubular linear reluctance motors (TLRMs), which can operate in different modes such as self- oscillating, switched-oscillating and accelerator. A tubular linear reluctance motor consists of two main parts: a moving part, and stator. The stator consists of an exciting coil that excites the magnetic field. Also, the moving part is a ferromagnetic material which is called plunger. The tubular linear reluctance motor in its simplest form is presented in Fig. 1 [6, 7].

A tubular linear reluctance motor is an electric motor in which velocity and magnetic force are produced by the tendency of its movable part (plunger) to move to a position where the inductance of the excited winding is maximized or the reluctance to the flow of magnetic flux is decreased. The resistance to the creation of magnetic flux in the material around the coil of the motor is called reluctance. Ferromagnetic material in the plunger reduces the reluctance and therefore magnetic force is developed due to the change in the reluctance of the material surrounding the coil as the plunger moves. The ferromagnetic plunger has a greater magnetic permeability than the air it replaces. As a consequence, the magnetic flux can be formed more easily when the plunger is centered on the coil. At this point, the reluctance is minimum for a given flux level; it is also the position of least energy. When displaced from the centered position, magnetic forces will always act to restore the plunger to its centered position.

The tubular linear reluctance motor is a series of coils activated sequentially to pull the plunger along the bore. Note that the plunger is only pulled, and is never pushed. This is a disadvantage of the TLRM when it is compared to other synchronous accelerators that can be pushed and pulled by choosing the relative polarity of the armature and stator windings.

Tomczuk and Sobol [6] investigated tubular linear reluctance motors (TLRMs) in various types of magnetic circuits. They analyzed magnetic field and calculated integral parameters of the field and also determined static characteristics and electromagnetic parameters of the motor. Also, in [7], the performance of the linear reluctance oscillating motor operating under ac and dc supply is investigated. Design of a reluctance accelerator and discusses the methods used in its design is described in [8]; it also discusses the methods of control of the accelerator and its predicted performance. In [9] Mendrela demonstrated the design and principle of operation and performance of a linear reluctance self-oscillating motor. This paper examined a mathematical model of a motor, permitting analysis of the dynamics and transients occurring in this circuit.

Many researches have been investigating TLRMs behavior, mostly focused on evaluation of TLRMs operation modes and structure. While, to our knowledge, no research has concentrated on calculating maximum inductance or profile inductance theoretically and in all the mentioned references, the minimum and maximum inductance is obtained by measuring method. Even it is mentioned in [10] that The dynamic inductance of the motors was not calculated on the basis of the magnetic field analysis. They often were obtained with using measured inductance only.

* Electrical Engineering Department, Iran University of Science and Technology (IUST), Iran University of Science and Technology, Narmak, Tehran, Iran, PO Box 1684613114, mosallanejad@iust.ac.ir

DOI: 10.2478/v10187-011-0035-x, ISSN 1335-3632

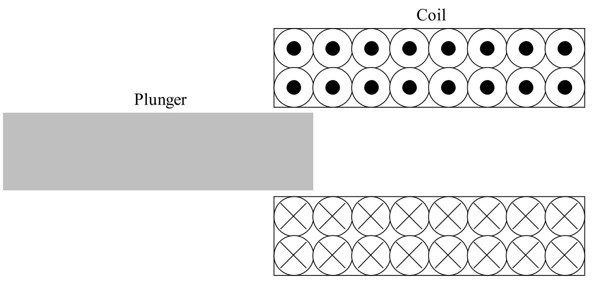

Fig. 1. Tubular linear reluctance motor with open magnetic system [4]

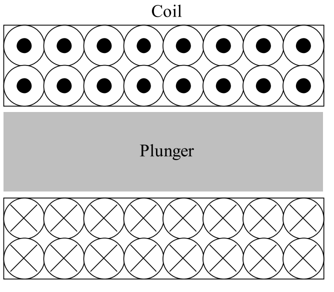

Fig. 2. Tubular linear reluctance motor with open magnetic system when the plunger placed in the centre of the coil

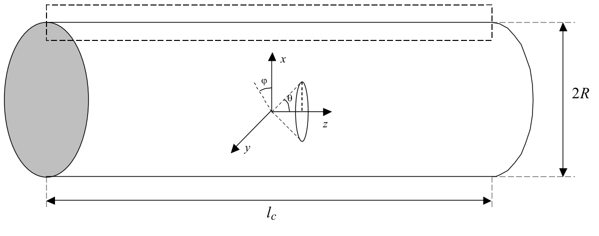

Fig. 3. Schematic of the iron core

In this paper, a new approach in maximum inductance calculation is proposed based on energy method. In energy method, it is necessary to calculate the field intensity inside the iron core. Furthermore, in order to calculate the maximum inductance, equivalent permeability is measured. Therefore, in this paper, field intensity inside the iron core is calculated with regard to eddy current. Finally, calculation, simulation, and experimental results of coil inductance are compared.

2 METHODS OF THE INDUCTANCE PROFILE CALCULATION

Operation of the tubular linear reluctance motor depends on the inductance profile of the machine. The machine inductance is related to machine dimensions such as the coil and plunger, excitation currents, and plunger position. Therefore, calculation of motor inductance with a good accuracy is very important. The winding inductance, L, is determined according to plunger position. Considering that the inductance of the coil is dependent on the position of the plunger, the inductance is estimated as follows

$$L = L_m\Big[1 + \cos\big(\frac{\pi}{l}x\big)\Big] + L_{\min}\,, \tag{1}$$

$$L_m = \frac{L_{\max} - L_{\min}}{2}\,, \tag{2}$$

where $L_{\min}$ is the inductance of the coil without the plunger and $L_{\max}$ is the inductance of the coil with the plunger placed in the centre of the coil, so that ($x = 0$). In other words, inductance should be determined in the presence ($L_{\max}$) and in the absence of the plunger ($L_{\min}$).

According to (1), inductance profile calculation is done for two different basic positions of plunger in this motor. The two positions take place when the coil is without the plunger or the plunger is fully inside the coil. The two aforementioned positions yield the minimum and maximum inductance, respectively. In other words, Eq. (1) receives the measured maximum and minimum inductances and estimates the inductance profile for the other positions. But our proposed method is able to calculate the coil inductance profile proportional to each plunger position.

There are many methods for calculation of coil minimum inductance. Most of them are experimental [12–17]. While, no methods are presented in literature to calculate the maximum inductance. But in this paper a new approach in maximum inductance calculation is proposed based on energy method.

2.1 Maximum Inductance Calculation

Applying electrical energy to the Tubular Linear Reluctance Motor, the plunger is pulled into the coil due to a strong magnetic field generated by a coil current. When plunger enters to coil, the inductance increases and reaches to its maximum value.

The coil inductance with the plunger placed in the centre of the coil, so that $x = 0$, is maximum that is shown in Fig. 2.

In this paper energy method is utilized in order to calculate the maximum inductance. The stored energy in an inductor is actually stored in its surrounding magnetic field. Hereby, an explicit formula for the stored energy in a magnetic field is obtained. The stored energy in the coil when a current I flows through the winding is as follows

$$W = \frac{1}{2}LI^2 \tag{3}$$

where L is the self-inductance. Also the stored energy in the solenoid can be rewritten as follows:

$$W = \frac{B^2}{\mu_0}V\,, \tag{4}$$

$$B = \mu_0\frac{NI}{l}\,, \tag{5}$$

where V is the volume of the solenoid. The above equations are simply used when coil is without the plunger.

If plunger enters the coil, it is necessary that the field intensity inside the iron core to be calculated.

Usually in electrical motors the iron core is laminated, while in TLRMs, it is integrated. Therefore, the high eddy current is produced inside the core.

Figure 3 shows a cylindrical core of the linear reluctance motors without coil. In Fig. 3, R is the cores radius and l_c is the length of the iron core. The current $i(t)$ in the winding flows in the ϕ direction of the cylindrical coordinate system shown in Fig. 3.

With flowing current in the coil, in one dimensional analysis, the flux line and the magnetic field intensity vector in the core has only the component along the z axis which depends only on the r coordinate along the cores radius and time, t, and the eddy current density vector has the ϕ-directed component $J_\phi(r,t)$ only. The Amperes circuital law is applied to a rectangular line consisting of a path located inside the iron core and the air gap (as indicated by the dashed line in Fig. 3). Therefore, we can write [11]

$$H_c(r,t)l_c + H_a(r,t)l_a = Ni(t) + l_c \int_r^R J_\theta(r,t)\mathrm{d}r\,, \quad (6)$$

where $H_c(r,t)$ and $H_a(r,t)$ are the magnetic field intensities in the iron core and in its related air gap, respectively. Also, l_a is the average length of flux path through the air gap.

Assuming $\phi_a = \phi_c$, we can write

$$H_a = \mu_{rc} H_c \frac{A_c}{A_a}\,. \quad (7)$$

In TLRMs, the flux path consists of two parts *ie* air gap and iron core. In (6), core length (l_c) is known but the average length of flux path through the air gap should be determined. The following formula is proposed to calculate l_a

$$l_a = \frac{\mu_0 Ni(t)}{B_c}\frac{A_c}{A_a} - \frac{I_c}{\mu_{rc}}\frac{A_c}{A_a}\,, \quad (8)$$

where μ_{rc} is the relative magnetic permeability of the iron core. Substituting (8) and (17) into (16) yields

$$\frac{\mu_c H_c(r,t)Ni}{B_c} = Ni(t) + l_c \int_r^R J_\theta(r,t)\mathrm{d}r\,. \quad (9)$$

In left side of (9), Ni can then be written in the form of

$$Ni(t) = Hl \quad (10)$$

and

$$H = \mu_e B_c \quad (11)$$

where μ_e is the equivalent magnetic permeability defined by [18]

$$\mu_e = \mu_0 \frac{\mu_{rc}}{1 + n(\mu_{rc} - 1)} \quad (12)$$

where

$$n \cong \frac{D_c^2}{l_c^2}\Big(\ln\frac{2l_c}{D_c} - 1\Big). \quad (13)$$

If the inner diameter of winding is equal to iron core diameter, then the above equation has a very high accuracy, otherwise its accuracy will be decreased; In TLRMs, (12) is not usable since there is air gap between plunger and coil; therefore in this paper, equivalent magnetic permeability (μ_e) is measured by the experimental results.

Substituting (11) and (10) into (9), Equation (9) can be rewritten in the form

$$\frac{\mu_c H_c(r,t)l}{\mu_e} = Ni(t) + l_c \int_r^R J_\theta(r,t)\,dr\,,\ 0 < r < R\,. \quad (14)$$

From (21), we can write

$$\frac{\partial H_c(r,t)l}{\partial r} = \frac{l_c}{l}\frac{\mu_e}{\mu_c}\frac{\partial}{\partial r}\Big[\int_r^R J_\theta(r,t)\mathrm{d}r\Big] = -\frac{l_c}{l}\frac{\mu_e}{\mu_c}J_\theta(r,t)\,. \quad (15)$$

Faradays law for the problem under consideration can be written as

$$\frac{\partial E_\phi(r,t)}{\partial r} = -\frac{\partial B_c(r,t)}{\partial t}\,. \quad (16)$$

Applying Ohms law and using (15) and (16),we can write

$$\frac{\partial^2 H_c(r,t)}{\partial r^2} = \frac{l_c}{l}\frac{\mu_e}{\rho}\frac{\partial H_c(r,t)}{\partial r}\,. \quad (17)$$

Equation (17) turns into the following equation for sinusoidal steady state conditions at an angular frequency of ω.

$$\frac{\partial^2 \widehat{H}_c(r)}{\partial r^2} = K^2\frac{\partial H_c(r)}{\partial r} \quad (18)$$

where

$$K = \sqrt{\frac{j\omega\mu_e l_c}{\rho_c l}} = \sqrt{\frac{l_c}{l}}\frac{1+j}{\delta_t} \quad (19)$$

and

$$\delta_t = \sqrt{\frac{\rho_c}{\pi\mu_e f}}\,. \quad (20)$$

The differential equation (18) has a general solution given by

$$\widehat{H}_c = \widehat{C}\cosh Kr\,. \quad (21)$$

Applying the boundary conditions to (21) yields

$$\widehat{H}(r) = H_{BO}\frac{\cosh(Kr)}{\cosh(KR)} \quad (22)$$

where $H_{BO}E$ is the magnetic field intensity phasor at the boundary of the core.

In order to calculate H_{BO}, using the differential form of the Maxwell–Faraday law, firstly we should calculate the eddy-current density phasor $\widehat{J}_\theta(r)$ in the core as in (23)

$$\widehat{J}_\phi(r) = (\nabla\times\widehat{H}_c(r))_\phi = - H_{BO}\sqrt{\frac{l_c}{l}}\frac{1+j}{\delta_t}\frac{\sinh\big(\sqrt{\frac{l_c}{l}}\frac{1+j}{\delta_t}r\big)}{\cosh\big(\sqrt{\frac{l_c}{l}}\frac{1+j}{\delta_t}R\big)}. \quad (23)$$

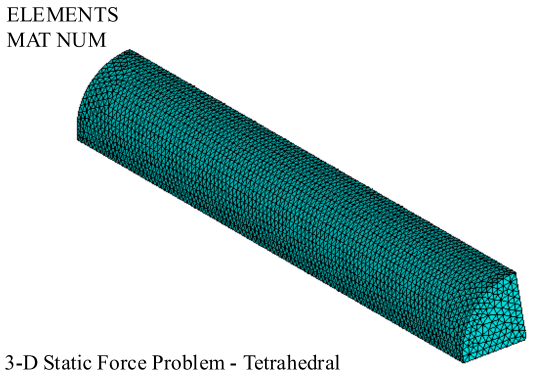

Fig. 4. The plunger model used in three dimension FEM

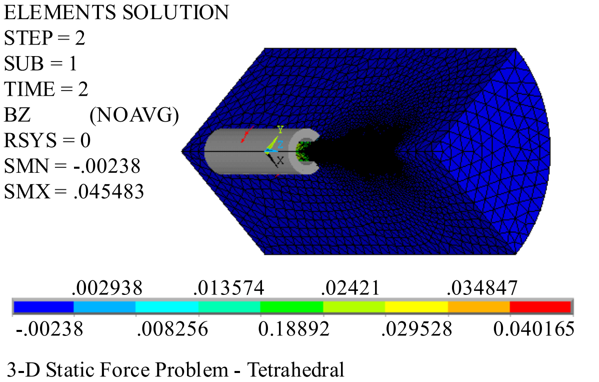

Fig. 5. Magnetic field density of motor when the plunger is located outside the coils

Substituting (23) into (14), and solving (14), the following relation is achieved

$$H_{BO} = \frac{\mu_e}{\mu_c}\frac{NI}{l}\,. \tag{24}$$

As previously mentioned, H_{BO} is the magnetic field intensity phasor at the boundary of the core and I is the phasor of the sinusoidal current flowing through the coil. Substituting (24) into (22), magnetic field intensities inside the iron core is achieved.

After determining field intensity inside the iron core, energy stored in the core can be calculated. When the plunger enters the coil as long as the distance of Δx, the stored energy is calculated from the following equation

$$W_m(x_0+\Delta x) = W_m(x_0) + \frac{1}{2}\frac{B_c^2}{\mu_e}S\Delta x \tag{25}$$

and

$$B_c = \mu_c H_c \tag{26}$$

where $W_m(x_0)$ is the coil energy stotage when the plunger is out of the coil. After substituting (24) into (26)and (26) into (25), the stored energy equation is

$$W_m(x_0+\Delta x) = \frac{1}{2}L_{\min}I^2 + \frac{1}{2}\mu_e\frac{N^2I^2}{l^2}S\Delta x\,. \tag{27}$$

When plunger enters the coil as long as the distance of x, the stored energy is obtained by integrating equation (27) from $0 \to x$ as the following

$$W_m(x_0+\Delta x) = \frac{1}{2}L_{\min}I^2 + \int_0^x \frac{1}{2}\mu_e\frac{N^2I^2}{l^2}S\Delta x\,. \tag{28}$$

Equation (28) can then be written in the following form

$$W_m(x_0+\Delta x) = \frac{1}{2}L_{\min}I^2 + \frac{1}{2}\mu_e\frac{N^2I^2}{l^2}Sx\,. \tag{29}$$

In (29), the first term on the right side is the coil energy with no plunger and the second one is the stored energy in the plunger. When the center of the plunger places in the centre of the coil, the stored energy in the coil is calculated by substituting $x = l_c$ in (29).

$$W_m(x_0+\Delta x) = \frac{1}{2}L_{\min}I^2 + \frac{1}{2}\mu_e\frac{N^2I^2}{l^2}Sl_c\,. \tag{30}$$

Equation (30) can be rewritten as:

$$\frac{1}{2}LI^2 = \frac{1}{2}L_{\min}I^2 + \frac{1}{2}\mu_e\frac{N^2I^2}{l^2}Sl_c\,. \tag{31}$$

Because the center of the plunger places in the center of the coil, the coil inductance is maximum, consequently (31) can be rewritten as

$$\frac{1}{2}L_{\max}I^2 = \frac{1}{2}I^2\Big(L_{\min} + \mu_e\frac{N^2}{l^2}Sl_c\Big). \tag{32}$$

According to Eq. (32), maximum inductance $L_{\max}$ is given by

$$L_{\max} = \Big(L_{\min} + \mu_e\frac{N^2}{l^2}Sl_c\Big) \tag{33}$$

where N is the coil turns, S is the cross section of plunger, l_c is the length of the plunger, l is the average length of flux lines path.

2.2 Calculation Inductance Profile

In that the coil inductance of the TLRM varies according to the position of the plunger, it is necessary to be able to calculate inductance of the coil at each position of plunger in order to model TLRM dynamically.

The most important feature of our proposed method is that it can calculate the coil inductance in each plunger position. For this purpose, substituting that length of the plunger which is inside the coil with l_c, the coil inductance in this position of the plunger is obtained.

3 CALCULATION OF MINIMUM AND MAXIMUM INDUCTANCE OF LABORATORY MODEL USING FEM

The basic geometrical data of the prototype of tubular linear reluctance motor is given in Tab. 1.

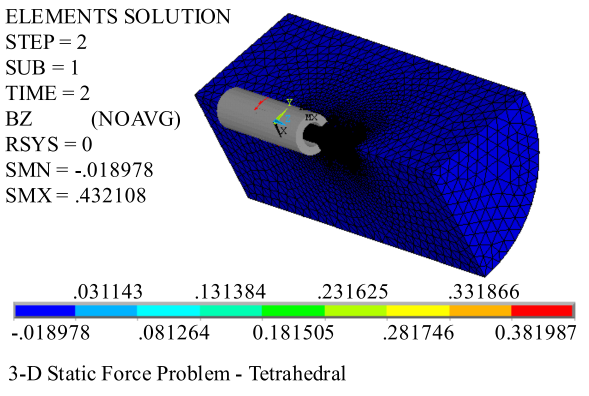

Fig. 6. Magnetic field density when the half of plunger is located inside the coils

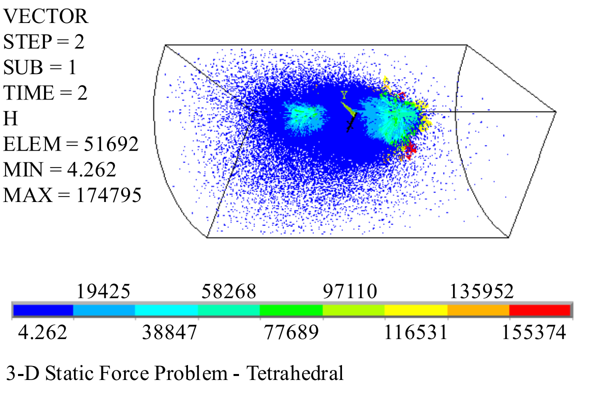

Fig. 7. Magnetic field intensity of motor when the plunger is placed in the center of the coil

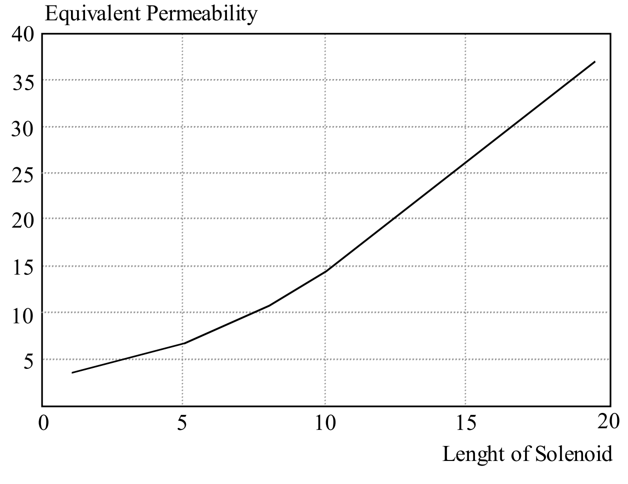

Fig. 8. Experimental measured equivalent magnetic permeability according to position of plunger

Table 1. Motor parameters

Symbol	Quantity	*Value*
N	Number of turn	710
D_{ci}	Coil inner diameter (mm)	40
D_{co}	Coil outer diameter (mm)	52
D_{po}	Plunger outer diameter (mm)	35
l_c	Length of plunger (mm)	200
l_w	Length of winding (mm)	200
μ_{rc}	Relative magnetic permeability	380
r	resistance coil (Ω)	0.98
d	Conductor diameter (mm)	0.0016

Because of axial symmetry of the plunger, the three dimension FEM analysis is done for a quarter of plunger area which is shown in Fig. 4.

In order to test the correctness of the proposed method, a tubular linear reluctance motor is modeled using 3-D FEM at a constant current during plunger motion. When plunger enters to coil, the inductance increases. While plunger moves inside the coils, the 3-D FEM measures the inductance. The results obtained by FEM are compared with the experimental results and the results obtained using the proposed method.

The magnetic field density of tubular linear reluctance motor when the plunger is out of the coil, is shown in Fig. 5. Simulation results of three dimension FEM analysis indicates that minimum inductance of tubular linear reluctance motor is about 3.8 mH.

When the half of plunger is inside the coil, inductance curve slope has the highest value. Due to the importance of this position, the motor is simulated by 3-D FEM in this position. The magnetic field density of this location is shown in Fig. 6.

According to three dimension FEM analysis a value of 28.7 mH is obtained for the coil inductance of tubular linear reluctance motor, when the half of plunger is inside the coil. Also the three dimension FEM analysis is done for calculation of the maximum inductance of tubular linear reluctance motor that is equal to 53.1 mH. The magnetic field intensity of tubular linear reluctance motor, when the plunger is placed in the center of the coil, is shown in Fig. 7.

Simulation results of three dimension FEM analysis indicates that the coil inductance and magnetic field density of tubular linear reluctance motor increases when the plunger is pulled into the coil.

The maximum inductance, calculated from proposed formula, is 51.1 mH. It should be mentioned that in order to calculate the maximum inductance from (40), the value of equivalent magnetic permeability should be determined. Since there is air gap between plunger and coil in TLRMs, equation (12) is not usable. Therefore, it is necessary to measure equivalent magnetic permeability (μ_e) experimentally. In this method, the coil voltage and current are measured, then the following formulas calcu-

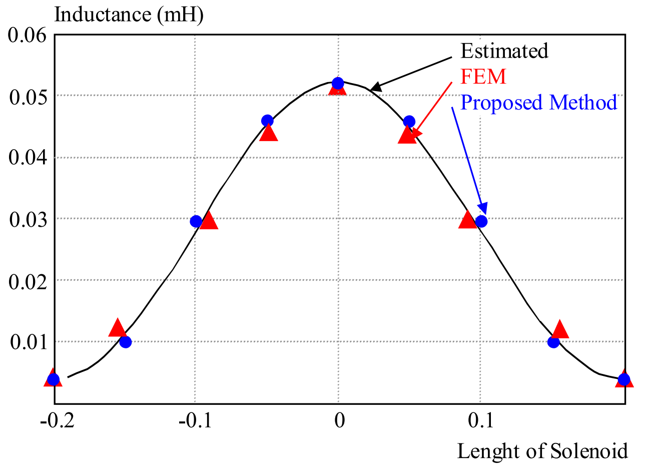

Fig. 9. Comparison of a simulation result with calculation wave form of coil inductance according to plunger position

Table 2. Simulation results using FEM, computational and experimental results

	Minimum Inductance (mH)	Maximum Inductance (mH)
Proposed Method	–	51.1
FEM	3.8	53.1
Experimental	3.95	51.5

late equivalent magnetic permeability (μ_e).

$$H = \frac{Ni}{l} \tag{34}$$

where N is the coil turns, l is the average length of flux lines path, H is the magnetic field intensity.

$$E = V - ir\,, \tag{35}$$

$$B_c = \frac{E}{4.44fNA_c}\,.$$

According to (26), equivalent magnetic permeability is given by

$$\mu_c = \frac{B_c}{H_c} \tag{36}$$

where E is the induced voltage in the coil, f is the power supply frequency, A_c is the core cross section.

The above test is done for all plunger positions and the equivalent magnetic permeability (μ_e) is measured for each position which is shown in Fig. 8.

In Fig. 8, equivalent magnetic permeability that measured from experimental results is shown for all position of plunger. If the coil is without the plunger, equivalent magnetic permeability is equal to that of air, but entering the plunger into the coil causes the equivalent magnetic permeability to increase and its value reaches to maximum when the plunger is completely inside the coil which is 35.7 as shown in Fig. 8.

4 EXPERIMENTAL RESULTS

Another method to determine minimum and maximum inductance is to measure them through the experiment. In this method, AC voltage is applied to the motor then current and voltage of motor are measured, in order to calculate minimum and maximum inductance. The above experiment should be implemented for both minimum and maximum inductances. According to this method, minimum and maximum inductances are 3.95 mH and 51.5 mH, respectively.

In Tab. 2, Simulation results using FEM, computational and experimental results are presented. As it is obvious in Tab. 2, the results of our proposed approach to calculate maximum inductance is close to simulation and experimental results and this shows that the proposed approach is accurate.

As mentioned before, in analysis of reluctance motor, the inductance of motor in any position of plunger is needed. Some research groups [4–10] have used Eq. (1) to estimate the inductance profile. This profile inductance is dependent on the minimum and maximum inductance of the coil. These literatures have used the measurement method to determine the maximum and the minimum inductance.

In this paper, however, we proposed a method which not only calculates the maximum inductance but also is able to calculate the inductance in any position of plunger. Figure 9 compares the results of the proposed method, the FEM results, and the results estimated using 1).

Comparing the results of proposed method, FEM analysis, and the inductance profile achieved by (1) clearly shows the ability of the proposed method in calculating the coil inductance in each plunger position.

5 CONCLUSION

Operation of the tubular linear reluctance motor depends on the inductance profile of the machine. Accuracy of coil inductance calculation in Tubular Linear Reluctance Motor facilitates precise prediction of motor behavior. The results of our proposed approach to calculate maximum inductance is close to simulation and experimental results and this shows that the proposed approach is accurate. The most important feature of the proposed method is its ability to calculate both the maximum inductance and the inductance profile in any position of the plunger. μ_e is the most important parameter for calculating maximum inductance that is measured from experimental results. Since there is air gap between plunger and coil in TLRMs, equation (12) is not usable. Therefore, in this paper, equivalent magnetic permeability (μ_e) is measured by the experimental results.

References

[1] NASAR, S. A.—BOLDEA, I.: Linear Electrical Motors: Theory, Design, and Practical Application, Prentice Hall, 1987.

[2] MARDER, B.: A Coilgun Design Primer, IEEE Trans. Magn. **29** No. 1 (Jan 1993), 701–705.

[3] LAITHWAITE, E. R.: A History of Linear Electric Motors, Macmillan, London, UK, 1987.

[4] BLAKLEY, J. J.: A Linear Oscillating Ferroresonant Machine, IEEE Trans. Magn. **MAG-19** No. 4 (July 1983), 1574–1579.

[5] NASAR, S. A.—BOLDEA, I.: Linear Electric Motors, Prentice Hall, Englewood Cliffs, 1987.

[6] TOMCZUK, B.—SOBOL, M.: Field Analysis of the Magnetic Systems for Tubular Linear Reluctance Motors, IEEE Trans. Magn. **41,** No. 4 (Apr 2005), 1300–1305.

[7] MENDRELA, E. A.: Comparison of the Performance of a Linear Reluctance Oscillating Motor Operating under AC Supply with One Under DC Supply, IEEE Transactions on Energy Conversion **14** No. 3 (Sep 1999).

[8] BRESIE, D. A.—ANDREWS, J. A.: Design of a Reluctance Accelerator, IEEE Trans. Magn. **27** No. 1 (Jan 1991), 623–627.

[9] MENDRELA, E. A.—PUDLOWSKI, Z. J.: Transients and Dynamics in a Linear Reluctance Self-Oscillating Motor, IEEE Trans. on Energy Conversion **7** No. 1 (March 1992).

[10] TOMCZUK—SOBOL: A Field-Network of a Linear Oscillating Motor and Its Dynamics Characteristics, IEEE Trans. on Magn. **41** No. 8 (Aug 2005).

[11] GRANDI, G.—KAZIMIERCZUK, M. K.—MASSARINI, A.—REGGIANI, U.—SANCINETO, G.: Model of Laminated Iron-Core Inducted for High Frequencies, IEEE Trans. on Magn. **40** No. 4 (July 2004).

[12] ALLGILBERLS, L. L.—BROWN, M. D.: Magnetocumulative Generators, Springer-verlag.

[13] HAGHMARAM, R.—SHOULAIE, A.—KHANZADEH, M. H.: Parallel Connection of Traveling Wave Tubular Linear Induction Motors, Proc. 3th Int. Conf. on Technical and Physical Problems in Power Engineering, Turkey, 2006, pp. 192–199.

[14] THORBORG—KJELD: Power Electronic, Prentice Hall, 1988.

[15] FOWLER, C. M.—CAIRD, R. S.—GARN, W. B.: An Introduction to Explosive Magnetic Flux Compression Generators, Los Alamos Report, LA-5890-MS, 1975, pp. 1–7.

[16] GROVER, L.: Inductance Calculations — Working Formulas and Tables, Dover, New York, 1962.

[17] CHENG, D. K.: Fundamentals of Engineering Electromagnetic, Addison-Wesley, 1993.

[18] TUMANSKI, S.: Induction Coil Sensors — a Review, J. Measurement Science and Technology **18** (Jan 2007).

Received 14 June 2010

Ali Mosallanejad was born in Jahroom, Iran in 1976. He received the BSc from Hormozgan University, Bandarabbas, Iran in 2002 , and MSc degrees from Iran University of Science and Technology (IUST), Tehran, Iran, in 2005. He is currently pursuing the PhD degree in electrical engineering at IUST. His research interests include power quality, power electronics, and electrical machines.

Abbas Shoulaie was born in Isfahan, Iran in 1949. He received the BSc degree from Iran University of Science and Technology (IUST), Tehran, Iran, in 1973, and the MSc and PhD degrees in electrical engineering from USTL, Montpellier, France, in 1981 and 1984, respectively. He is currently a Professor of Electrical Engineering at IUST. His research interests are power electronics, magnetic systems and linear motors, FACTS devices and HVDC.